

Blocked natural ventilation: the effect of a source mass flux

By ANDREW W. WOODS¹, C. P. CAULFIELD²
AND JEREMY C. PHILLIPS³

¹BP Institute for Multiphase Flows, University of Cambridge, Madingley Road, Cambridge, CB3 0EZ, UK

²Department of Mechanical and Aerospace Engineering, University of California, San Diego, 9500 Gilman Drive, La Jolla, CA 92093-0411, USA

³Centre for Environmental and Geophysical Flows, Department of Earth Sciences, University of Bristol, Bristol BS8 1RJ, UK

(Received 12 February 2002 and in revised form 4 April 2003)

We analyse the density evolution of fluid within a confined ventilated space resulting from the action of a dense turbulent plume originating at the top of the space with finite source volume flux, Q_0 , and initial source buoyancy flux, B_0 . The space is ventilated through upper and lower openings of areas A_u and A_l respectively, which are separated by a vertical distance H . We show that if $Q_0^3 < 2B_0Hc_l^2A_l^2$ (where c_l is an empirically determined discharge coefficient) then a two-layer steady stratification becomes established in the room, with outflow through the lower opening and inflow through the upper opening. The interface location depends not only on the geometry of the openings, but also the source conditions. We show that as Q_0 increases for fixed B_0 , the height of the interface, which equals the depth of the lower layer of relatively dense fluid, increases. Eventually, when the source volume flux has a value greater than $Q_m = (c_l A_l)^{2/3} (2B_0 H)^{1/3}$, the natural exchange flow becomes blocked and a steady outflow through both of the openings develops. As a result, the density of the fluid throughout the room gradually evolves towards the density of the incoming dense fluid. We compare our theoretical predictions with a series of laboratory experiments, and discuss the implications of our model for the design of ventilation systems.

1. Introduction

There has been considerable interest in the mixing produced by a localized source of buoyancy in a confined space since the pioneering work of Baines & Turner (1969). The problem is of central importance for modelling the natural ventilation of large buildings, where convective flows can dominate, and for processes such as Liquid natural gas (LNG) storage where the mixing of new, volatile-rich and older, volatile-poor LNG is crucial to avoid explosions (Germeles 1975). Mixing produced by a turbulent plume can also be important in open basaltic magma chambers in which new buoyant magma recharges the chamber from below (Phillips & Woods 2001). Baines & Turner (1969) examined the mixing produced by a plume in a confined region with initially uniform density. Their model focused on the motion of the so-called first front, which descends through the environment and across which there is an abrupt division between the original fluid in the room and the fluid which has been cycled through the plume. They also showed how the density profile of the

fluid behind this front could be determined by solution of the advection equation in the environment. This modelling was restricted to the idealized case of a pure source of buoyancy in which there is no source mass flux and in which there is only one opening. Linden, Lane-Serff & Smeed (1990) and subsequent workers extended the work to show that in a ventilated room, with two openings, a steady regime becomes established with inflow through one opening and outflow through the other (e.g. Cooper & Linden 1996; Gladstone & Woods 2001).

However, in many real applications, there is a non-zero mass flux associated with the source of buoyancy. Examples include a dense gas leak, hot-air underfloor heating and recharge in a magma chamber. Here, we show that such a mass flux can have a profound influence on the longer-term mixing and density evolution in a ventilated but otherwise enclosed space, where the ventilation prevents pressure build-up associated with the mass source. Caulfield & Woods (2002) have shown that with one opening, the flow in a ventilated filling box evolves away from that of the classical filling box, with the room becoming well-mixed and the density evolving approximately exponentially towards that of the incoming fluid.

Here we develop and apply this understanding to examine the case of a room with two openings. We find that if there is a sufficient source mass flux, then, as in Caulfield & Woods (2002), the room becomes well-mixed, with outflow through both openings. This corresponds to a purely mechanically ventilated regime. However, if the source of buoyancy has sufficiently small mass flux, then a two-layer steady stratification develops, with outflow through the lower opening and inflow through the upper opening (cf. Linden *et al.* 1990). We discuss the implications of these results for the design of natural ventilation systems. We describe the key result in §2, using a simple physical argument. In §3 we describe some laboratory experiments with which we have compared our physical model for the blocking of the natural ventilation. Section 4 describes the situation in which the natural ventilation does occur, and examines how the steady-state solution differs from that of Linden *et al.* (1990). In §5 we consider the case of high mass flux, and describe a simplified model to capture the evolution of this regime to a steady state. Finally, we discuss the applications of our results in §6, and draw some conclusions in §7.

2. Prediction of blocking

The flow regimes we consider are shown in figure 1, with figure 1(*a*) corresponding to the blocked flow regime, and figure 1(*b*) corresponding to the naturally ventilated flow regime. There is an isolated source of dense fluid which descends into the room from the top of the enclosed space. For simplicity we assume that the upper opening is located just below the ceiling and the lower opening is located just above the floor of the room. We also assume that the flow is unidirectional through each opening, consistent with our experimental observations for the range of flow rates and openings considered, and that the openings are of sufficiently small vertical extent that they may each be regarded as being located at a single depth within the room, and separated by a distance H .

We denote the initial specific buoyancy flux of this source as B_0 and the source volume flux as Q_0 , where

$$B_0 = \frac{g(\rho_s - \rho_a)}{\rho_0} Q_0 = g'_0 Q_0, \quad (2.1)$$

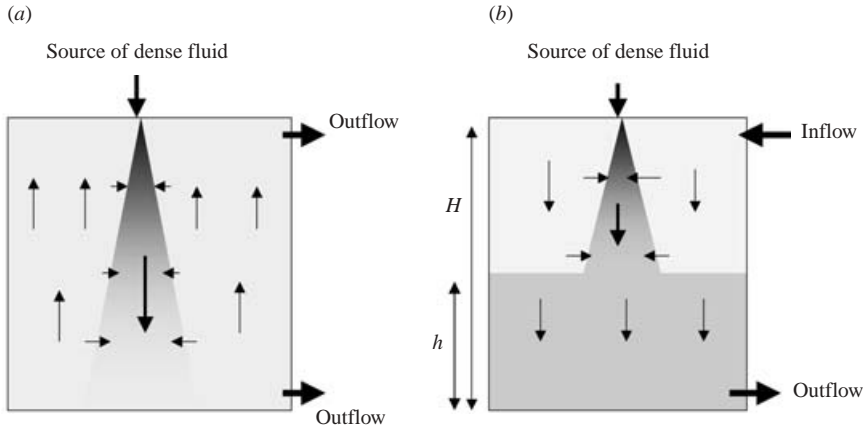


FIGURE 1. Schematics of the flow through a ventilated room with two openings and a source of mass and buoyancy: (a) the blocked flow; (b) the naturally ventilated flow.

ρ_0 is some reference density, ρ_s is the source fluid density, g'_0 is the initial source reduced gravity, and ρ_a is the external fluid density, which is assumed to be the same as the density within the room. The Boussinesq approximation is made so that the density variations from the reference density are only significant in calculating the buoyancy of the flow. Therefore, the results of this study are also directly applicable to buoyant plumes rising from the floor of a room, with openings at the floor and ceiling.

To understand how each of the two regimes may become established, we consider the development of the flow, assuming that the fluid in the room initially has the same properties as the exterior fluid. After the flow from the source commences, there will be outflow from both the upper and lower openings. However, as the turbulent buoyant plume develops from the dense source fluid, the density structure within the room will evolve. The plume entrains ambient fluid and convects the source and ambient fluid to the base of the room where it spreads out and forms a deepening layer of mixed fluid.

When the source mass flux is sufficiently large, as defined below, we expect that the deepening layer will ascend through the room, with the plume mixing the fluid throughout the room (figure 1a) as in the filling box process (Baines & Turner 1969). Indeed, Caulfield & Woods (2002) have shown that, owing to the finite volume flux, the density of the fluid within the room $\rho_r(z, t)$ then tends to become vertically uniform and gradually increases towards that of the source fluid ρ_s . As a result of the difference in hydrostatic pressure gradient inside and outside the room, the pressure difference between the interior and exterior fluid will become progressively larger at the lower opening compared to the upper opening. Therefore, an increasing fraction of the outflow tends to occur through the lower opening.

Indeed, if there is a pressure difference Δp between the interior and exterior of the room at the lower opening, then the volume flux through the lower opening Q_l is

$$Q_l = c_l A_l (2\Delta p / \rho_0)^{1/2}, \quad (2.2)$$

where c_l is a discharge coefficient for the opening, and A_l is the area of the opening (Linden *et al.* 1990). However, the outward flux through the upper opening Q_u has

the reduced value

$$Q_u = c_u A_u (2[\Delta p / \rho_0 - \overline{g'_r} H])^{1/2}, \quad (2.3)$$

where $\overline{g'_r}$ is the mean reduced gravity of the fluid in the room (with density $\rho_r(z, t)$) in comparison to the ambient external fluid (with constant density ρ_a), i.e.

$$\overline{g'_r} = \frac{1}{H} \int_0^H \frac{g(\rho_r - \rho_a)}{\rho_0} dz. \quad (2.4)$$

These two relations may be combined with the equation for the total conservation of mass

$$Q_l + Q_u = Q_0, \quad (2.5)$$

to show that

$$Q_u^2 = 2c_u^2 A_u^2 \left[\frac{Q_l^2}{(2c_l^2 A_l^2)} - \overline{g'_r} H \right]. \quad (2.6)$$

Equation (2.6) illustrates how the ratio of the fluxes through the upper and lower openings evolves as $\overline{g'_r}$ increases and more of the outflow occurs through the lower opening. The maximum value, $\overline{g'_m}$ say, that $\overline{g'_r}$ can attain occurs when the room is completely filled with source fluid. In this case, assuming that the room is initially filled with fluid of density ρ_a , it is apparent that

$$\overline{g'_r} \rightarrow \overline{g'_m} = \frac{g(\rho_s - \rho_a)}{\rho_0} = \frac{B_0}{Q_0} = g'_0, \quad (2.7)$$

the initial reduced gravity at the source. If (2.6) has a real solution for this limit, then using (2.7), we deduce that

$$Q_0 > Q_m = (2c_l^2 A_l^2 H B_0)^{1/3}, \quad (2.8)$$

and that there will be outflow through both openings. In the critical case in which $Q_0 = Q_m$ in (2.8) the flow through the upper opening is predicted to be zero once all the fluid originally in the room is replaced by source fluid, see (2.6). If $Q_0 < Q_m$, then we expect that at some point before all the fluid in the room has been replaced with source fluid, the flow through the upper opening will reverse, and a natural ventilation regime will become established (figure 1*b*). This is somewhat analogous to the flow predicted by Linden *et al.* (1990), except that they only considered the case of zero source mass flux. In order to test these predictions, we have conducted a series of laboratory experiments as described in the next section.

3. Laboratory experiments

We conducted a series of experiments to identify the transition from a blocked flow regime to the naturally ventilated regime as predicted by (2.8). Two rectangular Plexiglas tanks were used; the larger tank 2.0 m long \times 2.0 m wide \times 0.60 m deep provided a large reservoir of ambient fluid (fresh water) in which the smaller tank 0.18 m long \times 0.18 m wide \times 0.3 m deep was placed. The smaller tank had a vertical array of holes drilled in one side to act as openings into the larger tank.

The lowest hole was situated at the tank base, with 0.02 m spacing between the centres of the holes up to a height of 0.26 m. During an experiment, only the lowest hole and one other were open to provide top and bottom openings; the rest were sealed with rubber bungs. A purpose-built plume source was situated in the centre of the smaller tank with the source situated at the same level as the upper open hole.

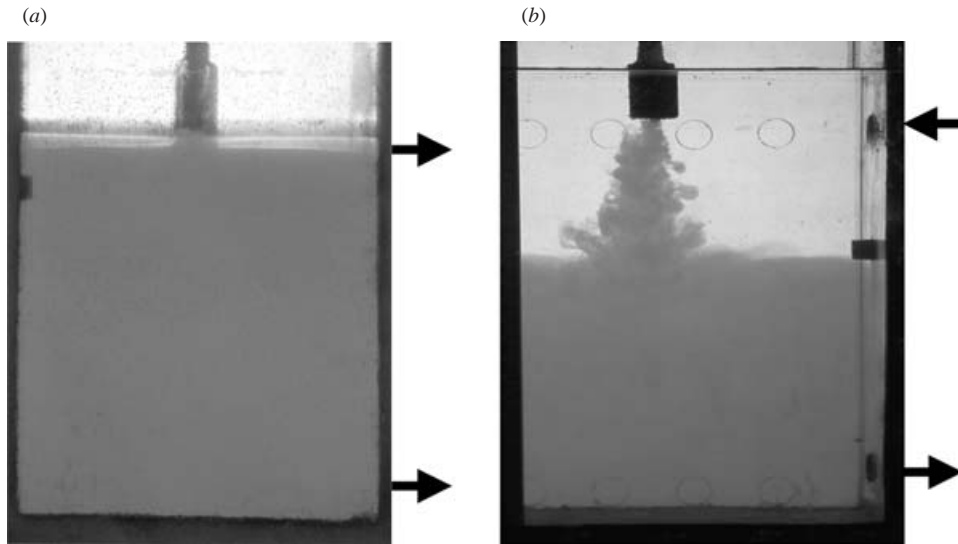


FIGURE 2. Photographs of two laboratory experiments exhibiting (a) the blocked flow and (b) the naturally ventilated regimes.

The plume source, of diameter 0.0045 m, discharged dense saline solution downwards into the smaller tank.

The nozzle design is similar to that of Dr Paul Cooper of the University of Wollongong, NSW, Australia, as described by Hunt & Linden (2001). For completeness, we note the key details below. The source consisted of a vertical tube of 0.007 m internal diameter and 0.005 m length. This tube opens into an expansion chamber of 0.011 m internal diameter and 0.025 m length. The upstream end of the chamber is connected to the outflow orifice by a 0.0006 m diameter hole. The final discharge occurs through a 0.0045 m circular orifice covered with 180 μm diameter nickel gauze. The vertical tube allows the flow to straighten, and then the flow through the expansion chamber reduces the momentum associated with the volume supply of fluid. Forcing the flow through the small hole triggers turbulent motions, which are augmented by the gauze at the downstream end of the chamber. Tests of this specific source show that the zone of flow establishment ahead of the source is very small, ≤ 0.005 m.

Experiments were conducted with the smaller tank initially filled with fresh (ambient) water. Dyed saline solution was introduced through the source and the resulting flow developed into a descending turbulent plume. For the lowest flow rate for which the plume was fully turbulent, a stable two-layer stratification developed within the smaller tank, with a sharp density interface between the layers (figure 2*b*; cf. Linden *et al.* 1990). The source flow rate was then increased, and a steady-state exchange was again set up between the smaller and larger tanks, but with a deeper lower layer of relatively saline fluid. By progressively increasing the flow rate, a series of steady interface heights was established, each corresponding to a particular source flow rate, until eventually the interface height just reached the height of the upper hole, and a weak outflow from the upper opening was observed. At higher flow rates, the blocked flow regime was observed (figure 2*a*).

Guided by the prediction (2.8) described in the previous section, a number of experiments were conducted to determine the critical flow rate for blocking, using

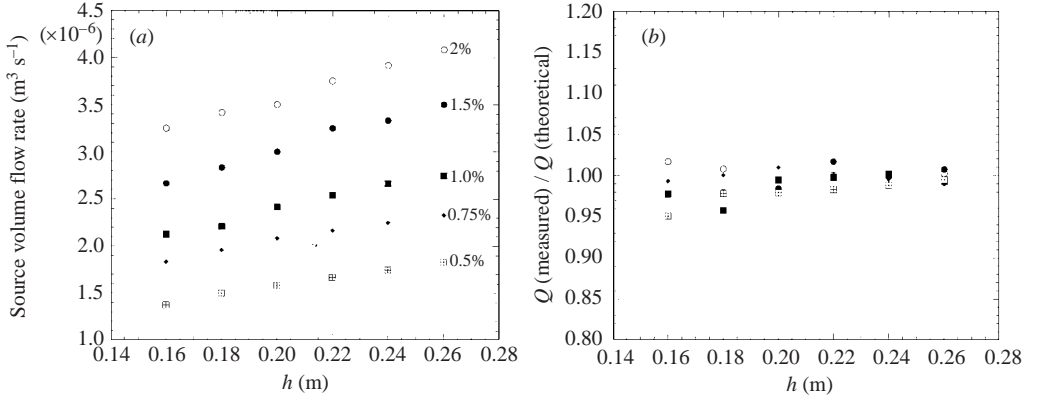


FIGURE 3. (a) The critical flow rate for blocking from 30 experiments, showing the dependence on the source volume flux and the initial density difference of the fluid. (b) The ratio of the experimental to theoretical value of the critical flow rate for blocking, as a function of the source volume flux.

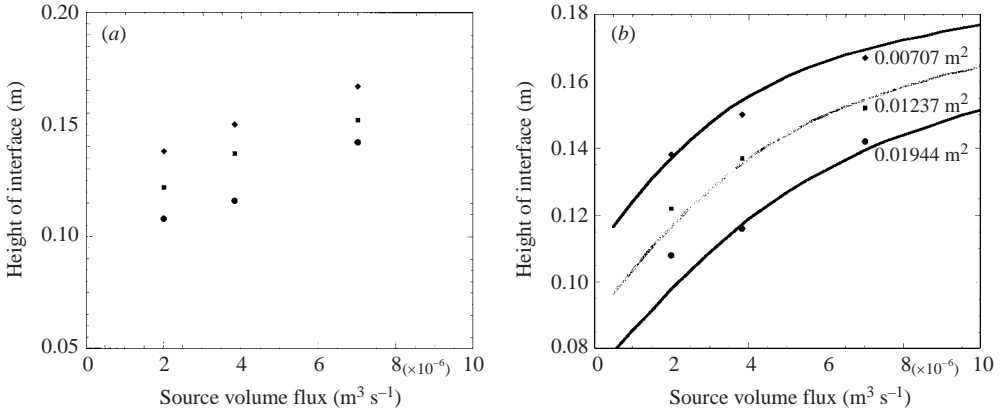


FIGURE 4. (a) The height of the interface as a function of the source volume flux. Experimental data are shown for three different flow rates and ventilation openings with areas 0.01944, (diamonds) 0.0123 (squares) and 0.00707 m^2 (circles). (b) Comparison of the model prediction of the interface height with the experimental data in (a).

five different saline solutions (0.5%, 0.75%, 1.0%, 1.5% and 2.0%) and six different spacings between the two openings (0.16, 0.18, 0.20, 0.22, 0.24 and 0.26 m). The dimensional values of Q_m are presented in figure 3(a), as a function of the distance between the openings, for the 30 different experiments, and the scaled value $Q_m / (2c_l^2 A_l^2 B_0 H)^{1/3}$ is shown in figure 3(b). It is seen that all the data collapse to the value 1 ± 0.05 , as suggested by the simple criterion for blocking, (2.8). In evaluating the theoretical prediction, we take the discharge coefficient for the flow through the opening to be $c_l = 0.7$, as determined by independent experiments (cf. Gladstone & Woods 2001).

Figure 4(a) shows the results of three sequences of experiments which illustrate how, prior to blocking, the height of the interface increases with source mass flux. In each of the experimental sequences, the source volume flux was gradually increased from 2×10^{-6} to 3.83×10^{-6} to $7 \times 10^{-6} \text{ m}^3 \text{ s}^{-1}$. In this case, the three experimental sequences correspond to three different areas of the ventilation openings: 0.01944,

0.01234 and 0.00707 m². In all these experiments the vertical distance between the openings was fixed at 20 cm. It is seen that there is a significant change (of the order of 20%–30%) in the interface height as the mass flux is increased by a factor of less than 3. In the next section, we develop a model to predict the height of the interface as a function of the source mass flux as well as the geometry of the room, and we compare this with the data shown in figure 4(a).

In a final series of experiments, the evolution of the density in the room during the blocking regime was measured by sampling fluid at different heights and times in the tank. The refractive index of these samples was measured using a Leica refractometer. The measurements were used to determine the salinity and hence density evolution of the fluid, and we discuss this in §5.

4. The natural ventilation regime: height of the steady-state mixed zone

Figures 1(b) and 2(b) illustrate the steady-state flow regime which becomes established for relatively small values of the source mass flux for which the natural ventilation flow dominates the effect of the source mass flux. There is a lower layer of density ρ_l and depth h above which lies a layer of the original ambient fluid (with density ρ_a). The upper layer is supplied by the inflowing fluid at the top opening, while the dense fluid exits from the lower opening.

Once again there is a pressure difference Δp between the interior and exterior of the room at the lower opening, and so the outflow volume flux at the lower vent is given by (2.2). In contrast to the model developed in §2 however, we now assume that there is inflow through the upper opening, of the form

$$Q_u = -c_{ui} A_u \left(2 \left[\frac{g(\rho_l - \rho_a)}{\rho_0} h - \Delta p / \rho_0 \right] \right)^{1/2} = -c_{ui} A_u (2[g_l' h - \Delta p / \rho_0])^{1/2}, \quad (4.1)$$

where $\rho_0 g_l' h$ represents the difference in the hydrostatic head inside and outside the room, owing to the well-mixed layer of fluid with reduced gravity g_l' and depth h at the base of the room, $Q_u < 0$ to denote inflow, and c_{ui} is the discharge coefficient associated with inflow through the upper opening.

At steady state, the buoyancy flux supplied by the source matches the buoyancy flux issuing from the lower vent, and so

$$Q_l g_l' = B_0 = Q_0 g_0'. \quad (4.2)$$

Using (2.2), (2.5), (4.1) and (4.2), the relationship between the outflowing flux, Q_l , and the height of the interface above the lower mixed layer, h , has the form

$$Q_l \left[Q_l^2 \left(1 + \frac{2c_{ui}^2 A_u^2}{2c_l^2 A_l^2} \right) + Q_0^2 - 2Q_l Q_0 \right] = 2c_{ui}^2 A_u^2 B_0 h. \quad (4.3)$$

These equations need to be supplemented by one further equation which quantifies the rate of mixing in the turbulent plume, and hence leads to a second relationship between Q_l and h . At the interface between the well-mixed lower layer and the upper layer of ambient fluid, the downward flux in the plume matches the net outflow from the room, Q_l . In general, the flow of the descending plume will involve a transition region near the source, before converging to self-similar plume flow in the far field, as described by Morton, Taylor & Turner (1956). If the vertical distance from the source to the density interface far exceeds the distance required for this adjustment, then use of the classical plume mixing model should provide a reasonable leading-order

estimate of the mixing (List 1982). Therefore, as an initial idealization to illustrate the key effects of the source mass flux, we assume that the material issuing from the source is in pure plume balance (cf. Caulfield & Woods 1995), and so is governed by the self-similar plume solution as described by Morton *et al.* (1956).

The plume theory predicts that the volume flux in the plume in an unstratified environment is

$$Q(z) = \lambda B_0^{1/3} (z + z_0)^{5/3}, \quad \lambda = \frac{6\epsilon}{5} \left(\frac{9\pi^2 \epsilon}{10} \right)^{1/3}, \quad (4.4)$$

where z is the distance from the real source, z_0 is the distance of the effective origin behind the source at which a pure source of buoyancy flux B_0 , with zero volume flux and zero specific momentum flux would produce an identical flow ahead of the real source, and ϵ is the 'entrainment constant' (Morton *et al.* 1956). Here, z_0 is given by the relation

$$Q_0 = \lambda B_0^{1/3} z_0^{5/3}. \quad (4.5)$$

The effective origin z_0 may be thought of as a parameter quantifying the relative importance of the source volume flux and the source specific buoyancy flux. Using this approximate model, it follows that the plume volume flux at the interface, a distance $H - h$ from the source (figure 1*b*), is given by

$$Q_p = \lambda B_0^{1/3} (z_0 + H - h)^{5/3}. \quad (4.6)$$

In steady state, the plume volume flux across the interface Q_p into the dense layer equals the flow of dense layer fluid Q_l out of the room. Therefore, combining (4.3) and (4.6), we obtain an implicit equation for h :

$$h = \frac{\lambda^3 y}{2c_{ui}^2 A_u^2} \left[y^2 \left(1 + \frac{2c_{ui}^2 A_u^2}{2c_l^2 A_l^2} \right) + z_0^{10/3} - 2z_0^{5/3} y \right], \quad y = (H - h + z_0)^{5/3}. \quad (4.7)$$

The density of the lower layer ρ_l can then be determined since, in steady state, the density in the plume when it arrives at the layer must be the same as the density of the layer, and so

$$\frac{g(\rho_l - \rho_a)}{\rho_0} = g'_l = \frac{g(\rho_s - \rho_a)}{\rho_0} \frac{z_0^{5/3}}{(H - h + z_0)^{5/3}} = g'_0 \frac{z_0^{5/3}}{y}. \quad (4.8)$$

In the limit $z_0 = 0$, (4.7) becomes

$$h = \lambda^3 (H - h)^5 \left(\frac{2c_l^2 A_l^2 + 2c_{ui}^2 A_u^2}{2c_l^2 A_l^2} \right), \quad (4.9)$$

which was originally presented by Linden *et al.* (1990) for the case of a pure source of buoyancy. In the other limit $h = H$, (4.7) reduces to the form

$$H = \frac{\lambda^3 z_0^5}{2c_l^2 A_l^2}, \quad (4.10)$$

and combining this with the definition of z_0 (4.5) we find that

$$Q_0 = (2B H c_l^2 A_l^2)^{1/3} = Q_m. \quad (4.11)$$

This coincides with the condition for blocking (2.8) derived in §2. For this critical case, the source strength $Q = Q_m$ requires that

$$z_0 = z_m = \left(\frac{2H c_l^2 A_l^2}{\lambda^3} \right). \quad (4.12)$$

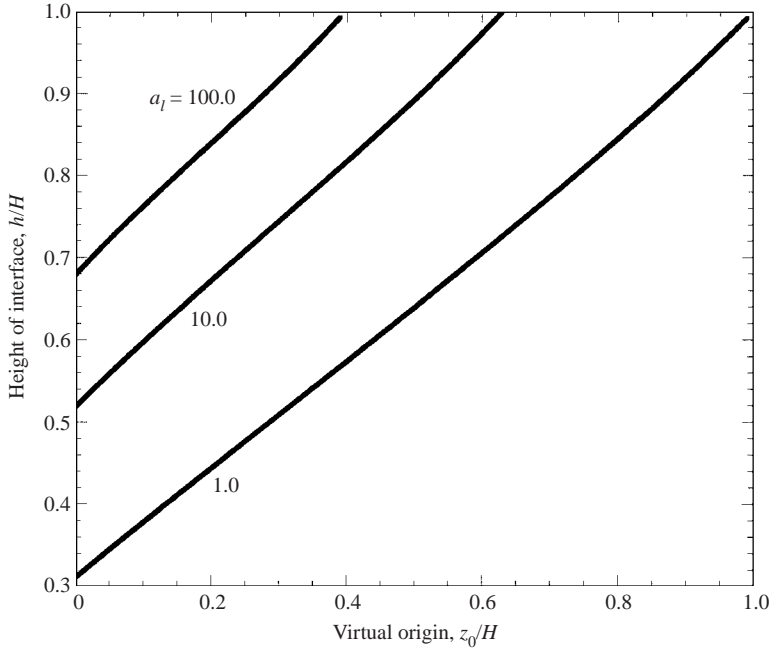


FIGURE 5. Prediction of the dimensionless height of the interface as a function of the parameter z_0/H , which determines the strength of the source volume flux relative to the source buoyancy flux, as defined in (4.5) and the geometrical parameter a_l as defined in (4.14), using (4.13) under the assumption that $c_{ui}A_u = c_lA_l$.

We have solved (4.7) numerically to find the solution for h/H as a function of z_0/H in the range $0 < z_0 < z_m$ and this is shown in figure 5. For simplicity, we assume that $c_{ui}A_u = c_lA_l$. In such a case, (4.7) can be re-posed in the straightforward dimensionless form

$$\hat{h} = \frac{h}{H} = a_l \hat{y} [2\hat{y}^2 + \hat{z}_0^{10/3} - 2\hat{z}_0^{5/3}\hat{y}], \quad (4.13)$$

where $\hat{y} = y/H$, $\hat{z}_0 = z_0/H$ and a_l is the geometric dimensionless parameter

$$a_l = \frac{\lambda^3 H^4}{2c_l^2 A_l^2}. \quad (4.14)$$

It is seen that the interface height increases with z_0 , until reaching the critical condition for blocking (4.12). Also, we see that the specific value of h increases as the ratio between the area of the lower opening and the square of the height of the room decreases. This reflects the reduction in the ventilation flow as the area of the openings decreases, and hence a tendency to reach blocking conditions more rapidly.

Although the value of z_0 depends on the specific source conditions, it increases monotonically with the source volume flux for a given source buoyancy flux. Equation (4.7) therefore illustrates that the height of the interface is dependent on the source volume flux. Conversely, z_0 decreases monotonically with source buoyancy flux for a given source volume flux, and so (4.7) also shows that the height of the interface is dependent on the source buoyancy flux. This is quite distinct from the case of an idealized pure source of buoyancy, with no associated mass flux, in which the height of the interface is independent of the source buoyancy flux. For real systems, such as an air-conditioning unit which supplies cool air, and in which the source buoyancy is

finite, the magnitudes of the effective source fluxes may be important in determining the location of the density interface in the room.

In comparing the theoretical model with measurements from actual experiments (figure 4), we need to estimate the rate of increase of volume flux in our experimental plumes with distance from the source. However, as the volume flux increases, or the area of the openings decreases, the interface tends to rise towards the top of the room, and therefore enters the near-source part of the descending plume. As a result, in the experiments, the plume motion may not have fully converged to the asymptotic law (4.4) which describes the volume flux as a function of the distance from the source.

In order to provide a more accurate comparison of the theory with our experiments, we have therefore solved the horizontally averaged equations describing the motion of a turbulent buoyant plume numerically. The two characteristic quantities of interest are the volume flux Q , and the specific momentum flux M , defined as

$$Q(z) = 2\pi \int_0^\infty w_p r dr = \bar{w}_p b^2, \quad M(z) = 2\pi \int_0^\infty w_p^2 r dr = \bar{w}_p^2 b^2, \quad (4.15)$$

where $w_p(r, z)$ and $\rho_p(r, z)$ are the axisymmetric, time-averaged vertical velocity and density distribution within the plume, ρ_r is the room density, ρ_0 is a reference density, g' is the reduced gravity, and we have defined, for simplicity, the equivalent top-hat values of the plume density $\bar{\rho}_p(z)$ and vertical velocity $\bar{w}_p(z)$, which are constant within the plume (of characteristic radius $b(z)$) and zero outside. In the unstratified region, $0 < z < h$, the buoyancy flux is constant $B = B_0$, and so Q and M satisfy

$$\frac{dQ}{dz} = 2\epsilon\pi^{1/2} M^{1/2}, \quad (4.16)$$

$$M \frac{dM}{dz} = B_0 Q, \quad (4.17)$$

where $\epsilon \simeq 0.12$ is an empirically determined entrainment coefficient or constant (Morton *et al.* 1956; Turner 1979, 1986) appropriate for top-hat models. Combining these relations, we find

$$\frac{dQ}{dz} = 2\pi^{1/2}\epsilon \left(M_0^{5/2} + \frac{5B_0}{8\pi^{1/2}\epsilon} (Q^2 - Q_0^2) \right)^{1/5}, \quad (4.18)$$

where Q_0 is the initial volume flux, and M_0 is the initial specific momentum flux. In our experiments, the flow issuing from the source had high Reynolds number and formed a turbulent flow so that to good approximation we assume

$$M_0 = \frac{Q_0^2}{A_s}, \quad (4.19)$$

where A_s is the source area.

We have integrated (4.18) numerically using the appropriate values of Q_0 , and hence M_0 using (4.19), for our experiments. Using this numerically determined relationship between Q_p and h combined with (4.3) and the observation that at steady state at the interface the plume volume flux Q_p equals the outflow through the lower opening Q_l , we can determine the steady height of the interface, h . Since the source conditions (4.19) are not in pure plume balance, this numerically determined value of h is somewhat different from the solution to the idealized, though instructive, implicit equation (4.7), though h exhibits the same qualitative dependence on Q_0 , B_0 , and the areas of the openings.

In figure 4(b) we present three curves which illustrate the predicted variation of the interface height with source volume flux, for the three values of the ventilation opening corresponding to the data in figure 4(a). It is seen that the difference between the theoretical prediction and experimental measurement is less than 10% for each particular experiment. However, there are insufficient data to confirm the overall trend of the predictions. It is worth noting that in figure 12(a) of Linden *et al.* (1990), the theoretical prediction of the interface height consistently overpredicts the experimental observation; although insufficient information is given in that paper to compare our model calculations with the data, the discrepancy may be related to the finite mass flux used in those experiments.

5. The blocked regime: evolution with time

For the blocked flow regime (figures 1a and 2a) there is outflow through both openings, and so the density of the interior continues to evolve until eventually the density matches that of the inflow. This evolution occurs with the interior fluid being, to a good approximation, well-mixed, in a similar manner to the evolution of the singly ventilated room, as described by Caulfield & Woods (2002). The mixing of the interior fluid occurs over a filling box time, which scales as

$$\tau_f = \frac{AH}{\lambda B_0^{1/3} H^{5/3}}, \quad (5.1)$$

where A is the cross-sectional area of the room. Subsequently, the density of the fluid venting from both openings is similar, and to leading order the mean reduced gravity in the room $\overline{g'_r}$, as defined in (2.4), may be described by a relation of the form

$$AH \frac{d\overline{g'_r}}{dt} = Q_0(g'_0 - \overline{g'_r}), \quad (5.2)$$

where g'_0 is the reduced gravity of the source fluid in comparison to the external ambient density of the incoming fluid, as defined in (2.1).

This equation has solution

$$\overline{g'_r}(t) = g'_0 \left[1 - \exp\left(\frac{-Q_0 t}{AH}\right) \right]. \quad (5.3)$$

In figure 6, we present a series of experimental data which illustrate how the dimensionless reduced gravity of the fluid in the room, $\overline{g'_r}(t)/g'_0$, varies as a function of the dimensionless time t/τ_r , where $\tau_r = AH/Q_0$ is the fluid replacement or turnover time, i.e. the time required to replace all the fluid in the room with input source fluid, in the complete absence of mixing. Data are shown for two experiments in which the buoyancy of the source fluid had value 2 wt% and 3 wt%. It may be seen in figure 6 that all the data collapses to the same curve, given by (5.3), supporting this very simple model of the density evolution of the interior in the fully blocked regime. The model applies as long as the filling-box time, τ_f , is much shorter than the fluid replacement time, τ_r , so that the layer becomes well-mixed prior to all the fluid being replaced by new fluid from the source. Caulfield & Woods (2002) have examined how the density profile evolves towards the well-mixed state in the analogous situation in which there is a single ventilation opening, considering arbitrary values of the ratio between these two times. The transient behaviour of the flow in the present case is

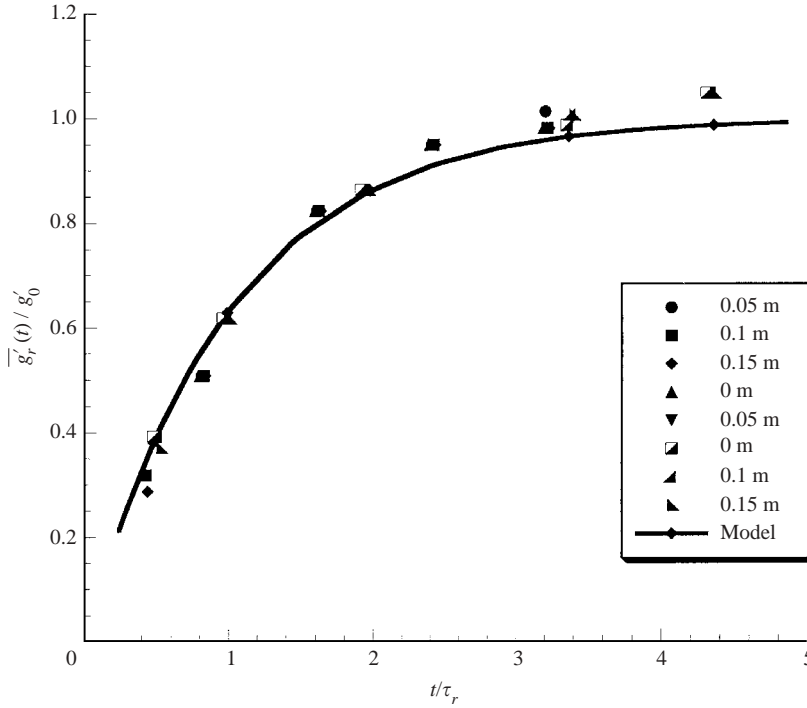


FIGURE 6. Variation of the reduced gravity in the room as a function of dimensionless time, for the blocked flow regime. Data are shown for two experiments, using source plumes with 2 and 3 wt% salt in solution. The source volume flux was $5 \times 10^{-6} \text{ m}^3 \text{ s}^{-1}$ for both experiments. Data are shown at four different depths in the room (0, 0.05, 0.10 and 0.15 m above the floor) for each experiment. The theoretical prediction using the simple well-mixed model given by (5.3) is also shown.

more complex, owing to the progressive evolution of the outflow through the two holes, and indeed some flows commence by being blocked but then become naturally ventilated. These effects are beyond the scope of the present contribution, and will be described in a companion paper, at present being prepared.

6. Application and discussion

The key result of this work is that when there is a source of mass as well as buoyancy, the natural ventilation regime may become blocked. According to (2.8), blocking is likely to occur if (i) the source mass flux is sufficiently large, (ii) the source buoyancy is sufficiently small, (iii) the area of the opening, through which there is outflow in the natural ventilation regime, is sufficiently small, or (iv) the distance between the two openings in the room is sufficiently small. It is curious that the size of the opening through which there is inflow during the naturally ventilated regime does not affect the critical condition for blocking. This is because at the critical condition there is zero net flow through that opening.

In order to illustrate how natural ventilation can enhance the volume flow of air through the room, in figure 7 we illustrate how (a) the total outflow from a room, and (b) the ratio of total volume outflow to the volume input from the cold source, vary with the volume input from the cold source, expressed as a function of the

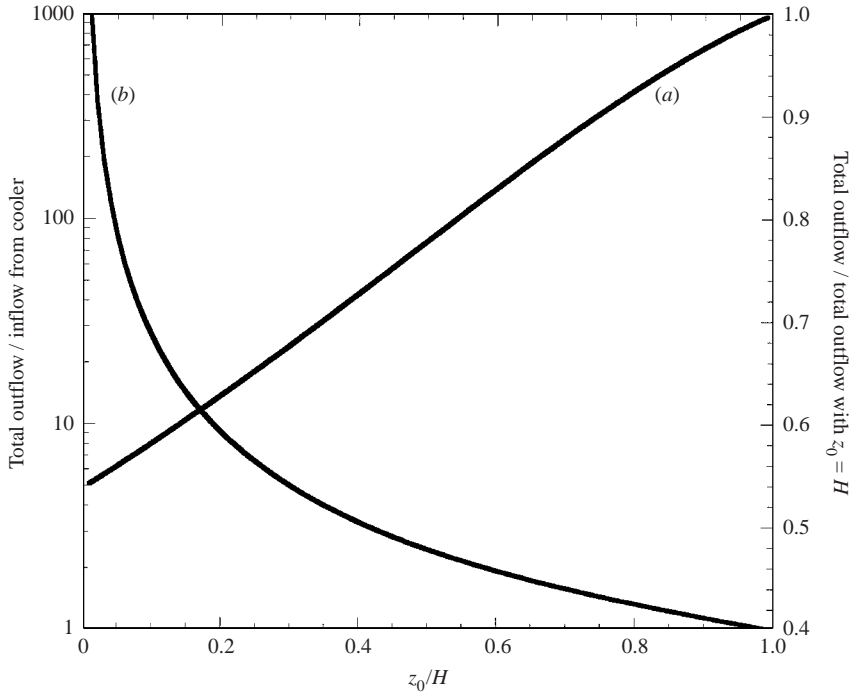


FIGURE 7. Evolution of flow rate in the natural ventilation regime, as the source mass flux, expressed through the virtual origin z_0 , changes. Curves illustrate the variation of (a) the total volume flux venting from the room, normalized by the value of the flux when $z_0 = H$; and (b) the ratio of the total volume flux venting from the room compared to the volume flow supplied by the cooling unit as a function of the effective virtual origin of the cooling unit. The curves illustrate how the natural ventilation can significantly enhance the circulation of air through the room, even though the total flow from the room decreases as the volume flux supplied from the chiller decreases.

effective origin of the source, z_0/H (§4). Figure 7 illustrates that as the source mass flux decreases (decreasing z_0), and hence the interface migrates downwards from the top of the room, the natural ventilation flow becomes progressively larger relative to the source mass flux, even though the overall volume flow decreases. Indeed, when the interface is located in the centre of the room, the natural ventilation flux is nearly 100 times greater than the flow supplied from the cooling unit. In this way, natural ventilation can provide a very effective means of maintaining circulation with a room, without the requirement to pump large quantities of air into the room.

We can use the blocking criterion (2.8) to understand conditions under which natural ventilation may develop in the situation in which cold air ventilates and chills a room, for example during summer. Let us consider the case in which the temperature difference between air-conditioned air and the exterior lies in the range 5–10 K, the area of the openings is 3 m^2 and the distance between the openings is 5 m. Then the reduced gravity of the cool air is of order $g'_0 = g\Delta T/T$ which has value $0.1\text{--}0.3 \text{ m s}^{-2}$. The critical flow rate for blocking given in (2.8) would then lie in the range $Q_m \simeq 2\text{--}3 \text{ m}^3 \text{ s}^{-1}$. For a room of volume $100\text{--}500 \text{ m}^3$, this would imply an overall fluid replacement time of about 2–3 minutes which is about 10 times greater than required; hence under such conditions, natural ventilation is a viable process.

The air conditioner could supply air at a slower rate to allow some natural ventilation to develop in the room, thereby enhancing the volume flow of air through the room relative to that purely associated with the cooler.

However, if the area of the ventilation openings was reduced to 0.3 m^2 , then the maximum critical flow rate of air from the chiller for the onset of natural ventilation would reduce to about $0.2\text{--}0.3 \text{ m}^3 \text{ s}^{-1}$. This would be close to the minimum flow required in order that the air in the enclosed space was replaced sufficiently frequently. Under such conditions natural ventilation may not be viable, since reducing the rate of supply of cool air from the chiller would reduce the overall flow from the room (figure 7), even if the natural ventilation suppresses the rate of decrease of ventilation flow relative to the supply from the chiller.

7. Conclusions

We have examined the situation in which a finite source of buoyancy of finite mass flux invades a reservoir which is ventilated through openings at two different levels (figure 1). The model has shown that a naturally ventilated two-layer stratification becomes established for small mass fluxes in an analogous fashion to that described by Linden *et al.* (1990). However, as the mass flux increases, the level of the interface between the two stratified layers advances towards the source of the buoyancy flux. As a result, the intensity of the flow through the opening nearer the source decreases towards zero. At this point, we describe the natural ventilation flow as being blocked. Any further increase in the source flux leads to outflow through both openings, and a cessation of the natural exchange flow. Our theoretical predictions have been confirmed by a series of analogue laboratory experiments which reproduce the conditions for blocking. We have also examined theoretically and experimentally (i) the steady-state flow regime which develops in the natural ventilation flow but accounting for the finite source mass flux, and (ii) the transient flow which develops for the blocked regime.

The modelling points to the important role of blocking in air-conditioned systems. When the exterior temperature is very high, the natural ventilation flow will tend to be dominant and leads to an exchange flow and a temperature stratification in the interior. With the blocked flow regime, the additional circulation of warm exterior air associated with natural ventilation is suppressed and ultimately leads to a cooler interior. In very hot conditions the blocked flow regime may therefore be preferable, while in more temperate conditions, natural ventilation flow may provide a very viable hybrid low-energy solution for ventilating the building, while cooling it with a chiller.

In closing we mention that there are several developments of this model which merit further investigation. As the aspect ratio of the room decreases so that the area of the plume becomes a significant fraction of the cross-sectional area of the room, then the mixing process will not be strictly described by the filling-box process and the interface height may therefore diverge from that in the present results. Also, if the source of buoyancy is not localized then the room will tend to become well-mixed and the stratification will be eroded (cf. Gladstone & Woods 2001).

This research has been funded in part by the EPSRC, the CMI Low Energy Building Project, the University of California Energy Institute, and the BP Institute. We are grateful to Gary Hunt for his suggestions about the design of the plume source used in our experiments.

REFERENCES

- BAINES, W. D. & TURNER, J. S. 1969 Turbulent buoyant convection from a source in a confined region. *J. Fluid Mech.* **37**, 51–80.
- CAULFIELD, C. P. & WOODS, A. W. 1995 Plumes with non-monotonic mixing behaviour. *Geophys. Astrophys. Fluid Dyn.* **79**, 173–199.
- CAULFIELD, C. P. & WOODS, A. W. 2002 The mixing in a room by a localized finite-mass-flux source of buoyancy. *J. Fluid Mech.* **471**, 33–50.
- COOPER, P. & LINDEN, P. F. 1996 Natural ventilation of an enclosure containing two buoyancy sources. *J. Fluid Mech.* **311**, 153–176.
- GERMELES, A. E. 1975 Forced plumes and mixing of liquids in tanks. *J. Fluid Mech.* **71**, 601–623.
- GLADSTONE, C. & WOODS, A. W. 2001 On buoyancy-driven natural ventilation of a room with a heated floor. *J. Fluid Mech.* **441**, 293–314.
- HUNT, G. R. & LINDEN, P. F. 2001 Steady-state flows in an enclosure ventilated by buoyancy forces assisted by wind. *J. Fluid Mech.* **426**, 355–386.
- LINDEN, P. F., LANE-SERFF, G. F. & SMEED, D. A. 1990 Emptying filling boxes: The fluid mechanics of natural ventilation. *J. Fluid Mech.* **212**, 300–335.
- LIST, E. J. 1982 Turbulent jets and plumes. *Annu. Rev. Fluid Mech.* **14**, 189–212.
- MORTON, B. R., TAYLOR, G. I. & TURNER, J. S. 1956 Turbulent gravitational convection from maintained and instantaneous sources. *Proc. R. Soc. Lond. A* **234**, 1–23.
- PHILLIPS, J. C. & WOODS, A. W. 2001 Bubble plumes generated during recharge of basaltic magma reservoirs. *Earth Planet. Sci. Lett.* **186**, 297–309.
- TURNER, J. S. 1979 *Buoyancy Effects in Fluids*, 2nd Edn. Cambridge University Press.
- TURNER, J. S. 1986 Turbulent entrainment: the development of the entrainment assumption, and its application to geophysical flows. *J. Fluid Mech.* **173**, 431–471.